Molecular Crystals and Liquid Crystals

ISSN: 1542-1406 (Print) 1563-5287 (Online) Journal homepage: http://www.tandfonline.com/loi/gmcl20

Detector-emitter system based on integrated organic vertical light emitting device and near-infrared organic photovoltaic cell

G. Barylo, V. Cherpak, G. Pakhomov, Z. Hotra, I. Helzhynskyy, M. Hladun, G. Wiosna-Salyga, B. Luszczynska & P. Stakhira

To cite this article: G. Barylo, V. Cherpak, G. Pakhomov, Z. Hotra, I. Helzhynskyy, M. Hladun, G. Wiosna-Salyga, B. Luszczynska & P. Stakhira (2016) Detector-emitter system based on integrated organic vertical light emitting device and near-infrared organic photovoltaic cell, Molecular Crystals and Liquid Crystals, 639:1, 177-185, DOI: 10.1080/15421406.2016.1255075

To link to this article: http://dx.doi.org/10.1080/15421406.2016.1255075

Published online: 14 Dec 2016.

MOLECULAR CRYSTALS AND LIQUID CRYSTALS
2016, VOL. 639, 177–185
http://dx.doi.org/10.1080/15421406.2016.1255075

Taylor & Francis
Taylor & Francis Group

Detector-emitter system based on integrated organic vertical light emitting device and near-infrared organic photovoltaic cell

G. Barylo[a], V. Cherpak[a], G. Pakhomov[b], Z. Hotra[a,c], I. Helzhynskyy[a], M. Hladun[d], G. Wiosna-Salyga[e], B. Luszczynska[e], and P. Stakhira[a]

[a]Lviv Polytechnic National University, Lviv, Ukraine; [b]Institute for Physics of Microstructures of the Russian Academy of Sciences (IPM RAS), RF Nizhny Novgorod, Russia; [c]Rzeszow University of Technology, Rzeszow, Poland; [d]European University, Lviv Branch, Ukraine; [e]Department of Molecular Physics, Lodz University of Technology, Lodz, Poland

ABSTRACT
We propose a new concept of the vertical exciplex-type organic light emitting structure with multilevel metallization that can serve as light-to-electricity-to-light convertor. The superimposition of operation and control voltages allows to tune the spectrum of the emitted light from blue to green, which is achieved by varying the potential applied to the device terminals or by illuminating the integrated organic Schottky diode employing a near-infrared absorbing titanyl phthalocyanine (TiOPc) dye.

KEYWORDS
OLED; organic photovoltaic cell; exciplex; infrared

1. Introduction

The progress in fluorescence imaging techniques for noninvasive visualization of biological processes in real time [1] requires search and realization effective instruments for visualization of the near infrared (NIR) emission and developing ways to determine the spatial localization of fluorophores markers in biological objects. Currently, there are implemented a number of approaches to create optoelectronic devices [1–6], among which, we believe, devices based on upconversion NIR into visible image [1] are the most promising in terms of ergonomics. Traditionally, these optoelectronic devices were realized using components of inorganic solid-state electronics [7], but substantial progress in the technology of organic displays [8], transistors [9], photovoltaics [10], photodetectors [11] memory [12], and bio-sensors [13] created the preconditions for the competitiveness of the latter to implement such instruments, due to the possibility of realization of flexible, large-area, and transparent devices by using low-cost techniques [3].

Phthalocyanines dyes are most frequently used in organic optoelectronic imaging device as detecting media due to their sensitivity to irradiation in the NIR range (650–900 nm) [1, 3, 5, 14–17]. Phosphorescent organic light emitting diodes (PHOLEDs) are used as element of visualization preferable because of their high efficiency and brightness [2, 4]. These systems have two significant disadvantages: 1) low contrast imaging (subjective perception of the intensity of luminescence OLED); 2) the high cost of iridium organometallic complexes [18].

CONTACT B. Luszczynska beata.luszczynska@p.lodz.pl
Color versions of one or more of the figures in the article can be found online at www.tandfonline.com/gmcl.

We propose a new approach to manufacturing integrated organic electronic devices incorporating the detector-emitter system for visualization of NIR irradiation. A distinct feature of such devices is a two-tone (depending on intensity) imaging in the NIR range. Basic element of such equipment is a three-terminal light-emitting device with adjustable emission color (blue and green) that can be driven by two independent voltages. Driving of the individual OLED is made by a signal originating from preliminary conversion and processing of photo-signal from organic photodetector. Signal information component is determined by the intensity of detected infrared radiation, resulting in a change in both intensity and spectrum emission of the OLED structure.

Green color is due to emission from the highly efficient organic light emitting structure of exciplex type (4,4′,4″-tris[3-methylphenyl(phenyl) amino]triphenylamine (MTDATA): 2,8-bis(diphenylphosphoryl) dibenzo[b,d]thiophene (PPT)) [19] in which the intramolecular spin up-conversion from non-radiative triplet state to the radiative singlet state (thermally activated delayed fluorescence (TADF)) [19, 20] is realized and is characterized by the high values of the external quantum efficiency (10%) [19]. Blue color is due to highly efficient exciton and excimer emission from m-MTDATA [21, 22].

2. Experimental

The device consists of three functional parts: i) light-emitting imaging system, ii) reception system for the near infrared (NIR) radiation, and iii)electrical circuit for processing and conversion of the detected signal.

2.1. Fabrication of vertical organic light-emitting imaging system

The electroluminescent vertical device (Fig. 1) was fabricated by thermal evaporation of organic semiconducting layers and metallic electrodes onto pre-cleaned ITO-coated glass substrates under a vacuum of 10^{-5} mbar. The cleaning procedure included consecutive ultrasonic treatment in different solvents. The layer of m-MTDATA acts thereby as hole-transporting (donor) and blue light-emitting layer, the PPT layer as electron-transporting (acceptor) layer, which in combination with the m-MTDATA layer (in between of the interdigitated electrodes) leads to the appearance of the above mentioned green exciplex emission at the organic-organic interface [19].

The electrical characteristics were measured using a semiconductor parameter analyzer (HP 4145A) and two source measuring units (SMUs) [23]. When the voltage was applied to the inserted thin-film Ca:Al electrodes, the interdigitated electrodes were connected together.

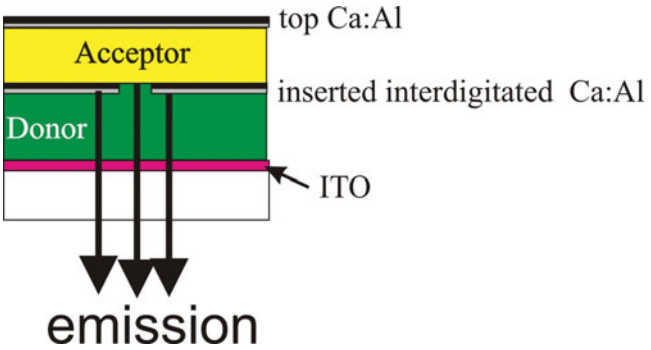

Figure 1. Schematic presentation of fabricated organic light emitting transistor device.

The electroluminescence spectra were recorded with an Ocean Optics USB2000 spectrometer. All measurements were performed at ambient conditions.

2.2. Fabrication of photo-sensitive detector for infrared radiation

The NIR detecting part was fabricated and tested using the methods and facilities described previously [24]. Due to high photosensitivity of TiOPc in NIR spectra region [25–27] initial TiOPc powder (dye content >95%, Aldrich) was routinely sublimed onto pre-cleaned ITO-coated glass substrates under a vacuum of 10^{-5} mbar to obtain thin polycrystalline layers (phase II, thickness 35 nm). Next, strip Al electrodes (60 nm) were thermally evaporated on the surface of TiOPc layers through the shadow mask. The peak photocurrent intensity of thus fabricated detector corresponds to the incident light wavelength of 850 nm.

2.3. The development of electrical circuit for processing and conversion of detected signal

Proceeding from the preliminary studies on organic photosensor and vertical light emitting structure (see above), we developed the generalized functional control scheme. This scheme (Fig. 8) consists of the blocks for amplification and processing of incoming information (signal photodetector). We assembled operational amplifier, comparator, pulse-width modulator and driver for organic light emitting structure to implement the scheme. Formation of dual-channel output voltage for the OLED vertical structure supply (change in radiation color) depending on the input information signal from the photodetector is done by operational amplifier and comparator. Change in the brightness of the radiation is done using a controlled pulse width modulator.

3. Results and discussion

3.1. Study of radiation color switching and current flow in the vertical light- emitting structure

In the Fig. 2, the equivalent scheme of the fabricated devices is shown.

Diode A (ITO/CuI/m-MTDATA/PPT/topCa:Al) – is a high efficient green emitting exciplex-type device, its band diagram is shown in Fig. 3a.

Diodes B,B' (ITO/CuI/m-MTDATA/interdigitated Ca:Al) – is a blue emitting device, its band diagram is shown in Fig. 3b.

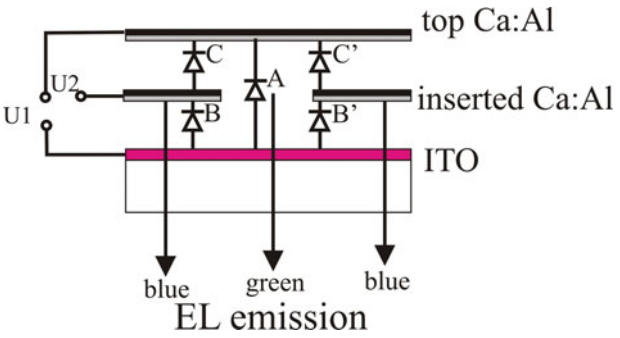

Figure 2. Equivalent scheme of fabricated devices.

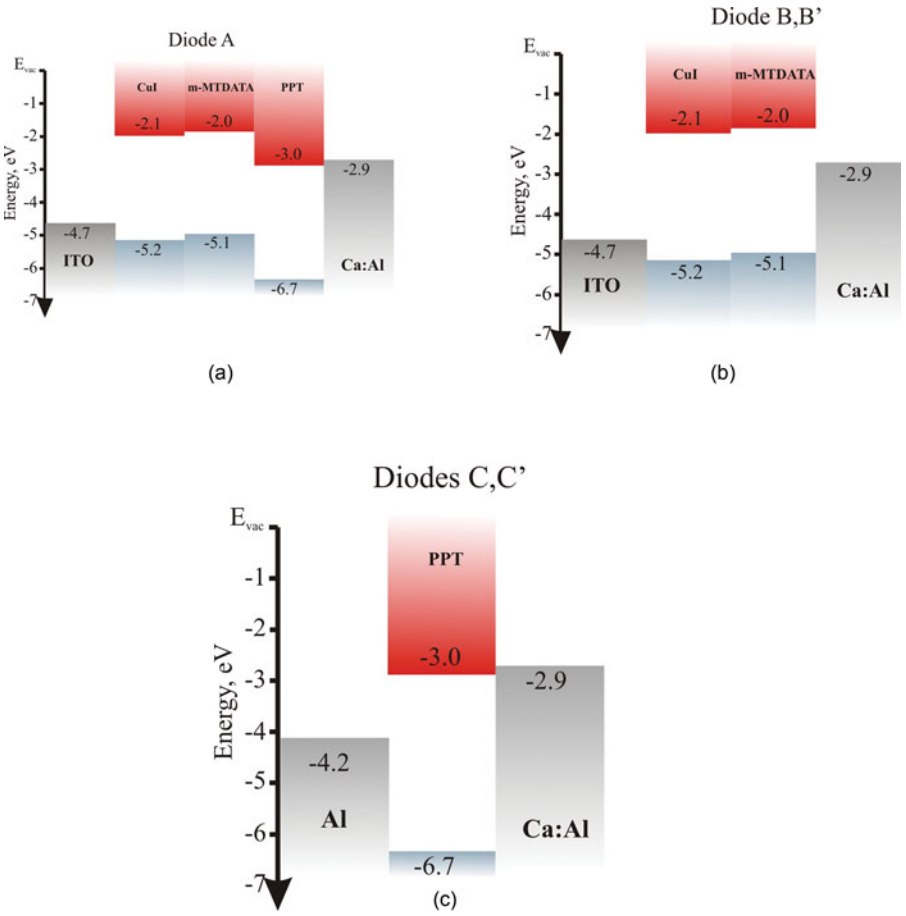

Figure 3. Energy diagrams of device components.

Diodes C,C' (interdigitated Ca:Al/PPT/topCa:Al) - are "electron only" devices, the band diagram is shown in Fig. 3c.

Output characteristic of fabricated device are shown in Fig. 4.

As seen from the output characteristics (Fig. 4), current between ITO and top Ca:Al electrodes increases (similarly to the current flow between drain-source electrodes in the conventional OFET structure), with increasing negative potential applied to the inserted electrodes relative to the top metal electrode (analogs of source-gate). When applying the positive potential to the inserted electrode relative to the top metal electrode, the current between the upper ITO and Ca:Al electrodes decreases (Fig. 4).

It should be noted that the drain-source current is not only the current of exciplex type diode (A). It is essentially a superposition of currents flowing across the structure of the device, thus the current value is affected by redistribution of the charge withinthe whole structure.

3.2. *Simulation of device operation*

We carried out the simulation of the device operation based on combinational circuit of internal elements for structure. Simulation of the main modes of operation is carried out using a Proteus software. We used a dual-channel measuring system (channel 1 and channel 2) to

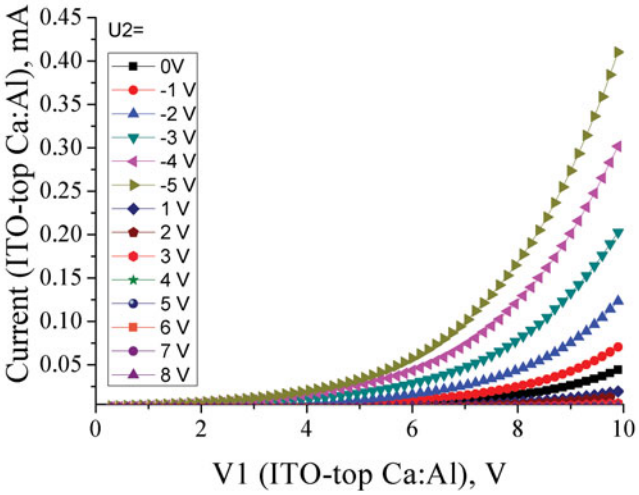

Figure 4. Output characteristic of fabricated device at the different applied value of U2 (n- negative potential applied to inserted Ca:Al electrode, p- positive potential applied to inserted Ca:Al electrode).

analyze the current-voltage characteristics of the elements. In this case, channel 1 simulates applying a voltage between ITO and the upper metallic electrode (top Ca:Al), channel 2 – between the top and middle metal electrodes (interdigitated Ca:Al).

High current efficiency of exciplex type diodes [19] in comparison with the exciton diodes leads to significant differences between the current flowing through diodes A and B. This feature is used to set up the functional diodes' models, in this case operating current of diode A is an order of magnitude lower than current of diode B.

Emission color of the device is determined by the turn-on voltage of light emitting diodes A and B. In this case, due to higher energy barriers in the structure of blue diodes (B), their turn-on voltage is higher compared to the exciplex-type diode (A).

Thus, if the applied voltage U1 is higher than 5V, and in absence of applied voltage to inserted electrodes, then a green emission from the exciplex-type diode A is observed (see Fig. 6a and Fig. 7). If the applied voltage U1 increases to 6 V, or applied voltage U2+U1>6V, two different emissions can be observed simultaneously.

Let us consider the main operation modes of the devices.

1. U1 is higher than switching-on voltage for exciplex OLED (U1 = 5 V), U2 = 0 B (actually, it is short circuit for channel 2), and we observe luminescence of exciplex diode A (Fig. 5a, Fig. 6 (curve B)).
   In this case the voltage-current dependence I1(U1) is typical for OLED [19]. The characteristics reflect the total current through two barrier structure of exciplex (A) and exciton (B) type, as shown in Fig. 7 curve 1.
   The experimental I-V dependence (Fig. 7) is mainly determined by the current flow through a layer of m-MTDATA, while diode B is in a pre-threshold switching-on state. This mode corresponds to a characteristic point on the experimental current-voltage curve (Fig. 7, 1).
2. U1 is higher than switching-on voltage for exciplex OLED (U1 = 5 V), U2 = 1 V ("+" is connected to the middle metallic electrode, "–" is connected to the top metallic electrode), and we observe the luminescence of exciplex diode A (Fig. 5b, Fig. 6 (curve A)). We have to note that in this mode the current through diode A is not changed, while the current through B reduces since the voltage on it is defined as the difference between

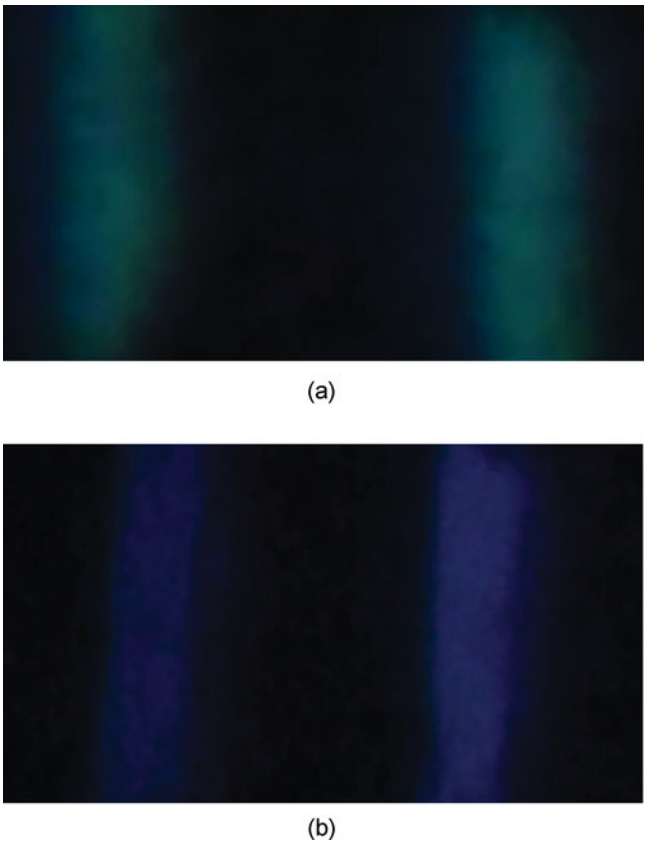

Figure 5. Photos of green (a) and blue (b) emitting regions of device.

the applied voltages U1 and U2 (4 V). This mode corresponds to a characteristic point on the experimental current-voltage curve (Fig. 7, 2).

3. U1 is higher than switching-on voltage for exciplex OLED (U1 = 5 V), U2 = −1 V ("+" is connected to the top metallic electrode, "–" is connected to the middle metallic

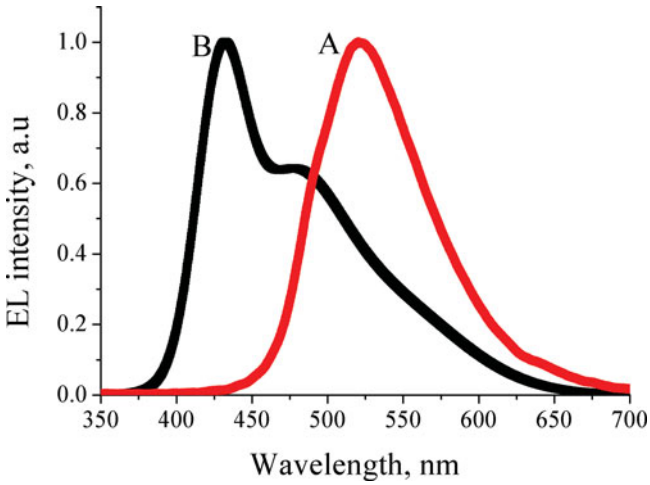

Figure 6. EL spectra from two type of emission from diodes A and B.

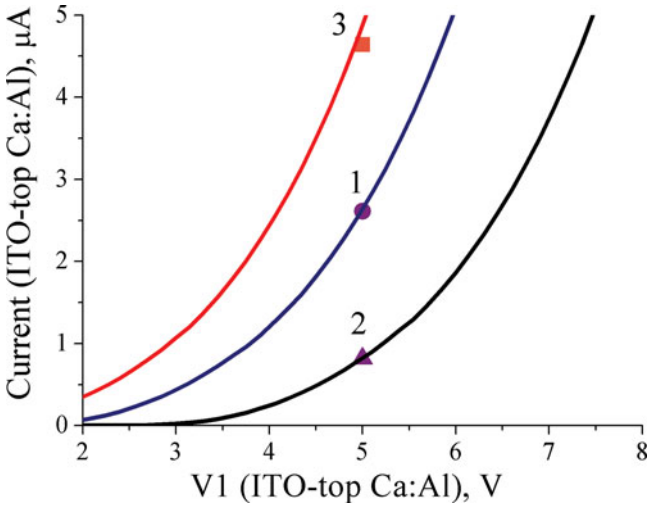

Figure 7. Experimental I-V curves and fitted points.

electrode). In this mode we observe luminescence of diodes of both exciplex diode A and exciton diode B type. As in the previous case, the current through diode A is not changed, while the current through diode B increases because the voltage drop on it is defined as the sum of the applied voltages U1 and U2 (6V), that is higher than switching-on voltages for exciton type diode B. This mode corresponds to a characteristic point on the experimental current-voltage curve (Fig. 7, 3).

4. The applying of negative voltage that is higher switching-on voltage for exciton OLED (U2 = 6 V) and U1 = 0 V (actually, it is a short circuit for channel 2) causes an unexpected experimental result – appearance of the exciton luminescence. In this case the voltage of channel 2 through the short-circuited channel 1 is applied directly to the diode B, while diode A is shunted by short-circuited input of channel 1.

3.3. Fabrication of a hybrid electronic device for imaging the intensity of the NIR irradiation by integrating organic light-emitting and photosensitive structures

Schematic block diagram of the hybrid electronic devices for visualization of the intensity of the NIR irradiation is shown in Fig. 8. The operational principle of the proposed device is as follows: infrared irradiation with a fixed intensity is detected by the organic photodetector (OPD) and then the resulting electrical signal is amplified by operational amplifier (OA).

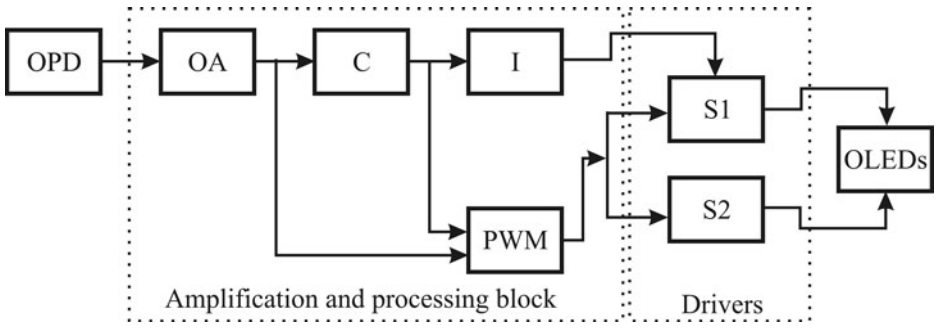

Figure 8. Block diagram of the hybrid electronic devices for NIR visualization.

Formed by OA voltage level, obtained according to the function of optical conversion and amplification, is a sublinear dependence of the intensity of the light flux on the output voltage values which lie between 0 and U_{max}. With the comparator (C) two sub-bands of voltage in the range 0- $U_{max}/2$ and $U_{max}/2$- U_{max} are formed. The first sub-band corresponds to the low comparator output voltage, second, respectively, corresponds to the high voltage of comparator output. Switch (S1) is turned on by the low voltage of invertor (I) by transformation of low voltage level, as results the voltage from Pulse Width Modulator (PWM) is applied to output U1 of the organic light-emitting structure (OLEDs). Switch (S2) is turned on by the high voltage of comparator, which corresponds to the second sub-band, and the voltage from PWM is applied to output U2 PWM provides the brightness control of the structure radiation with respect to the intensity of the input optical signal, taking into account the state of the comparator, selected band.

The increase in the intensity of the NIR irradiation causes the increase in radiation intensity of one OLED and subsequent switching of the second OLED with the same grow of radiation intensity. Voltage limits that correspond to the intensity of the input optical signal and the OLED threshold switching can be set according to the required sensitivity of the device.

Conclusion

New method of the spectrum tuning of organic light emitting device based on integration of OLED and NIR OPV was shown. The main feature of organic light emitting part of integrated device is indirect (NIR signal) control of the emission color in the vertical exciplex-type organic light emitting structure. It was suggested to use principle of color switching OLED according to changing of the intensity of NIR irradiation, on the base of carried out simulation procedure. Thus constructed integrated device provides a two-color highly-informative identification of the NIR signals and can be used in fluorescence imaging techniques for non-invasive visualization of biological processes.

Acknowledgment

Partial financial support for this research work, awarded by RFBR #15-08-06364.

References

[1] Guo, Z., Park, S., Yoon, J., & Shin, I. (2014). *Chem. Soc. Rev.*, *43*, 16.
[2] Kim, D. Y., Song, D. W., Chopra, N., De Somer, P., & So, F. (2010). *Adv. Mater.*, *22*, 2260.
[3] Liu, S. W., Lee, C. C., Yuan, C. H., Su, W. C., Lin, S. Y., Chang, W. C., & Chen, K. T. (2015). *Adv. Mater.*, *27*, 1217.
[4] Liu, S.-W., Li, Y.-Z., Lin, S.-Y., Li, Y.-H., & Lee, C.-C. (2016). *Organ. Electron.*, *30*, 275.
[5] Kaneko, M., Taneda, T., Tsukagawa, T., Kajii, H., & Ohmori, Y. (2003). *Jpn. J. Appl. Phys.*, *42*, 2523.
[6] Lv, W., Zhong, J., Peng, Y., Li, Y., Luo, X., Sun, L., Zhao, F., Zhang, J., Xia, H., Tang, Y., Xu, S., & Wang, Y. (2016). *Organ. Electron.*, *31*, 258.
[7] Welsher, K., Liu, Z., Sherlock, S. P., Robinson, J. T., Chen, Z., Daranciang, D., & Dai, H. (2009). *Nat. Nanotechnol.*, *4*, 773.
[8] Tang, C. W., & Vanslyke, S. A. (1987). *Appl. Phys. Lett.*, *51*, 913.
[9] Liu, S.-W., Su, T.-H., & Li, Y.-Z. (2014). *Org. Electron.*, *15*, 1990.
[10] Peumans, P., & Forrest, S. R. (2001). *Appl. Phys. Lett.*, *126*, 126.
[11] Gong, X., Tong, M., Xia, Y., Cai, W., Moon, J. S., Gao, Y., Yu, G., Shieh, C. L., Nillsson, B., & Heeger, A. J. (2009). *Science*, *325*, 1665.
[12] Zhou, Y., Han, S. T., Chen, X., Wang, F., Tang, Y. B., & Roy, V. A. L. (2014). *Nat. Commun.*, *5*, 4720.

[13] Guo, Z., Park, S., Yoon, J., & Shin, I. (2014). *Chem. Soc. Rev.*, *43*, 16.
[14] Pakhomov, G. L., Travkin, V. V., Luk'yanov, A. Yu., Stakhira, P. I., & Kostiv, N. V. (2013). *Tech. Phys.*, *58*, 223.
[15] Pakhomov, G. L., Pakhomov, L. G., Travkin, V. V., Abanin, M. V., Stakhira, P. Y., & Cherpak, V. V. (2010). *J. Mater. Sci.*, *45*, 1854.
[16] Afify, H. A., El-Nahass, M. M., Gadallah, A.– S., & Khedr, M. A. (2015). *Mater. Sci. Semicond. Process*, *39*, 324.
[17] Tanaka, H., Yasuda, T., Fujita, K., & Tsutsui, T. (2006). *Adv. Mater.*, *18*, 2230.
[18] Xiao, L., Chen, Z., Qu, B., Luo, J., Kong, S., Gong, Q., & Kido, J. (2011). *Adv. Mater.*, *23*, 926.
[19] Goushi, K., & Adachi, C. (2012). *Appl. Phys. Lett.*, *101*, 023306.
[20] Dias, F. B., Bourdakos, K. N., Jankus, V., Moss, K. C., Kamtekar, K. T., Bhalla, V., Santos, J., Bryce, M. R., & Monkman, A. P. (2013). *Adv. Mater.*, *25*, 3707.
[21] Graves, D., Jankus, V., Dias, F. B., & Monkman, A. (2014). *Adv. Funct. Mater.*, *24*, 2343.
[22] Ivaniuk, K., Chapran, M., Cherpak, V., Barylo, G., Stakhira, P., Hotra, Z., Hladun, M., & Dudok, T. (2015). *Ukr. J. Phys. Opt.*, *16*, 95.
[23] Cherpak, V., Gassmann, A., Stakhira, P., Volyniuk, D., Grazulevicius, J. V., Michaleviciute, A., Tomkeviciene, A., Barylo, G., & von Seggern, H. (2014). *Org. Electron.*, *15*, 1396.
[24] Travkin, V. V., Stuzhin, P. A., Okhapkin, A. I., Korolyov, S. A., & Pakhomov, G. L. (2016). *Synth. Met.*, *212*, 51.
[25] Wang, W., Placencia, D., & Armstrong, N. R. (2011). *Org. Electron.*, *12*, 383.
[26] Mayukh, M., Macech, M. R., Placencia, D., Cao, Y., Armstrong, N. R., & McGrath, D. V. (2015). *ACS Appl. Mater. Interfaces*, *43*, 23912.
[27] Obata, N., Sato, Y., Nakamura, E., & Matsuo, Y. (2011). *Jap. J. Appl. Phys.*, *50*, 121603.